Lagrangian Chaos: Transport, Coupling and Phase Separation

Thomas H. Solomon, Nathan S. Miller, Courtney J. L. Spohn, and Jeffrey P. Moeur

Bucknell University
Lewisburg, PA 17837 USA

Abstract. We present results of experimental and numerical studies of Lagrangian chaos (chaotic advection) in an oscillating vortex chain. We first review previous experiments on enhanced diffusive and superdiffusive transport in this flow. Superdiffusion occurs only as a transient and only at certain well-defined resonant frequencies. At these frequencies, long "flights" are found numerically in the trajectories with lengths with scaling similar to that of Lévy flights. We then discuss on-going experiments of the effects of Lagrangian chaos on more complicated dynamical processes occurring in this flow. Specifically, we study the dynamics of coupled Belousov-Zhabotinsky chemical oscillators in the oscillating vortex chain. We analyze the system as a network with each vortex and its contents forming the nodes of the network. Coupling between the nodes then is via Lagrangian chaos. With Lagrangian chaos, there is either nearest neighbor coupling (enhanced diffusion) or long-range coupling (superdiffusion and Lévy flights) which could make this system an experimentally-realizeable "small world" network. Three different modes of synchronization are found: unsynchronized oscillations, traveling waves, global "blinking" states, and a state in which lobes responsible for enhanced transport mediate the synchronization.

INTRODUCTION

It is well known that simple, laminar fluid flows can have surprisingly complicated mixing properties. Even if the velocity field itself is very well-ordered and deterministic, the trajectories of fluid elements or impurities in the flow may follow chaotic trajectories in the sense that nearby trajectories will separate exponentially in time [1,2]. There have been several studies of the effects of Lagrangian chaos on the mixing of passive impurities (e.g., miscible dyes). An important outstanding question, however, is how the presence of Lagrangian chaos affects *dynamical* processes occurring in a fluid flow.

In this article, we present the results of experimental and numerical studies of Lagrangian chaos in a simple two-dimensional flow composed of a chain of alternating vortices that sways periodically in the lateral direction. We start by discussing the nature of the chaotic mixing in this oscillating vortex chain and how this chaotic behavior affects long-range transport. We then discuss on-going experiments on coupled chaotic oscillators in this fluid flow and how Lagrangian chaos affects the global dynamics and synchronization of these coupled oscillators.

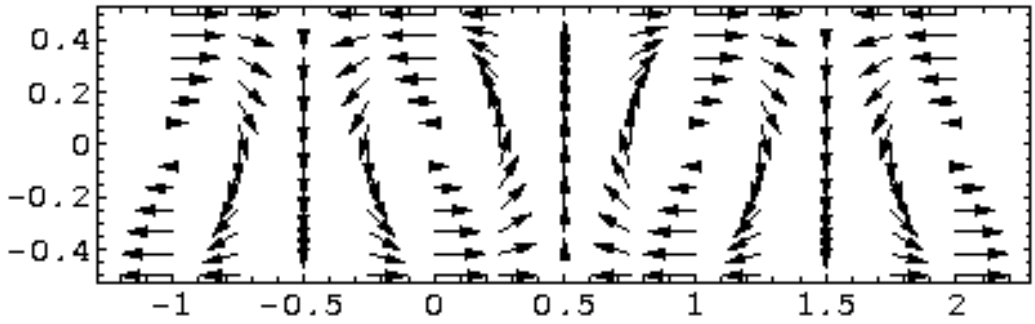

FIGURE 1. Alternating vortex chain for case with free-slip boundary conditions. The no-slip case would look similar, except that the velocities would vanish at the top and bottom boundaries. Time dependence is manifested as lateral oscillation of the entire velocity field with an amplitude B and an angular frequency ω.

MODEL FLOW AND EXPERIMENTAL TECHNIQUES

The flow studied is a chain of alternating vortices, as shown in Fig.1. This system was originally proposed as a two-dimensional cross-section of oscillatory (time-periodic) Rayleigh-Bénard convection [3-5]. In fact, experiments on time-periodic Rayleigh-Bénard convection demonstrated the presence of Lagrangian chaos [4]. Numerically, a simple model was proposed for this flow, based on the following streamfunction [6]:

$$\psi(x,y,t) = \frac{A}{k}\sin\{k[x + B\sin\omega t]\}W(y). \qquad (1)$$

The term $B\sin\omega t$ denotes the lateral oscillation of the vortex chain. We will scale the oscillation amplitude by the vortex width w; from hereon, we will denote the amplitude by this non-dimensional $b \equiv B/w$. For a flow with stress-free boundary conditions,

$$W(y) = \sin(\frac{\pi y}{d}), \qquad (2)$$

and for a flow with rigid (no-slip) boundary conditions,

$$W(y) = \cos(q_0 y) - A_1\cosh(q_1 y)\cos(q_2 y) + A_2\sinh(q_1 y)\sin(q_2 y), \qquad (3)$$

where q_o = 3.973639, q_1 = 5.195214, q_2 = 2.126096, A_1 = 0.06151664 and A_2 = 0.103887 [7]. The velocity field can be obtained by applying Hamilton's equations of motion to this streamfunction:

$$\dot{x} = \partial\psi / \partial y; \dot{y} = -\partial\psi / dx . \quad (4)$$

Numerical simulations [4,5] of particle trajectories in this flow demonstrate Lagrangian chaos denoted by trajectories that separate exponentially in time.

We have recently assembled an experimental configuration that generates this flow using a magnetohydrodynamic technique [8,9], as shown in Fig. 2. An electrical current passing through a thin (2 mm) electrolytic solution (salt water or dilute sulfuric acid) interacts with an alternating magnetic field produced by a chain of alternating Nd-Fe-Bo magnets underneath the fluid layer. Lorentz magnetic forces resulting from this interaction produces alternating horizontal forcing in the fluid layer which, in combination with the plexiglass side walls, produces the alternating chain of vortices. Time dependence is imposed externally with a plunger that oscillates slowly up and down, displacing the fluid laterally across the fixed pattern of vortices.[1] This system has an advantage experimentally over time-periodic Rayleigh-Bénard convection in that it allows independent control of both the amplitude and frequency of the lateral oscillations.

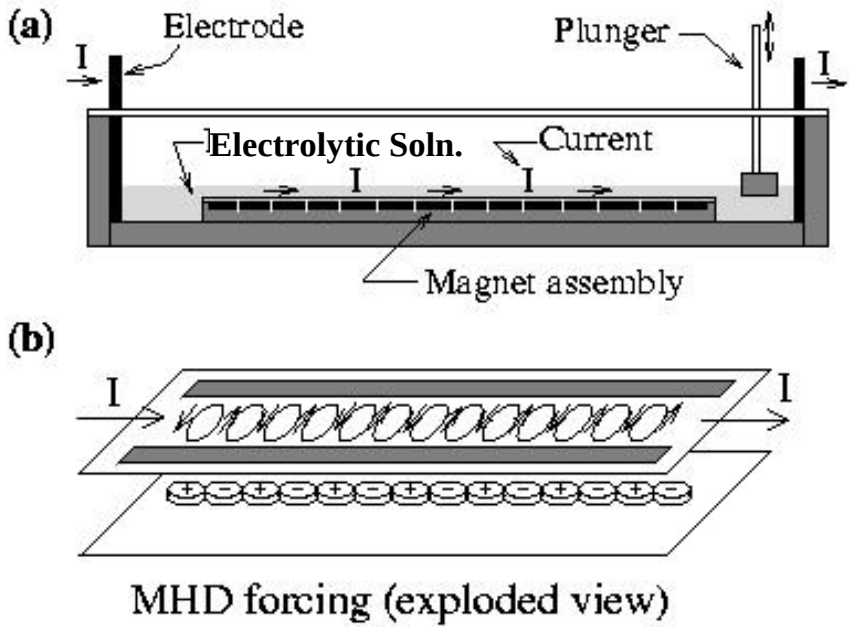

FIGURE 2. Diagram of experimental apparatus. (a) Side view; (b) exploded view showing magnetohydrodynamic (MHD) forcing technique.

For transport measurements, fluorescent dye is injected into the center vortex, and the system is illuminated with black light. The entire apparatus is imaged from above with a CCD video camera, and the images are digitized and analyzed on a PC-compatible computer.

[1] The period of oscillation is chosen to be several times the viscous diffusion time (~4 s) for the fluid layer. This is important to avoid "frozen" oscillations of the vortices which would be different kinematically from the model in Equations (1) – (3).

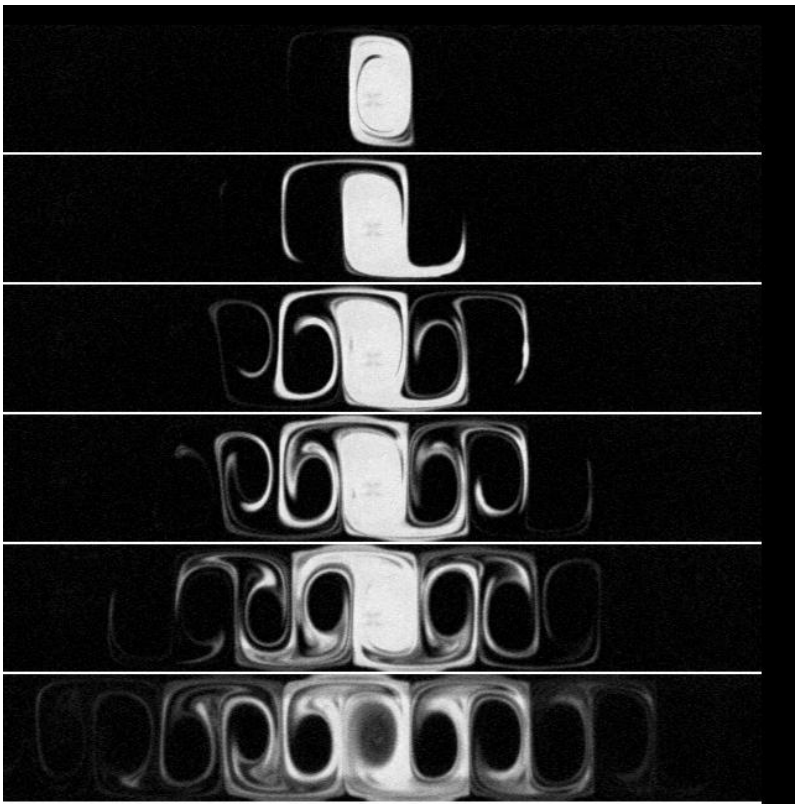

FIGURE 3. Sequence showing the mixing of dye due to Lagrangian chaos in the oscillating vortex chain; amplitude of oscillation b = 0.12; oscillation period = 19 s; time (from the top): 0, 1, 2, 3, 4 and 10 periods of oscillation.

ENHANCED TRANSPORT OF PASSIVE TRACERS

A sequence of images showing transport of a miscible dye is shown in Fig. 3. Several important features are visible: (a) A significant amount of stretching and folding is seen, typical of chaotic processes. (b) "Lobes" of dye (and clear fluid) are exchanged between adjacent vortices in the chain. This is the primary mechanism for mixing between the vortices [9,10]. (c) Ordered regions are visible in the vortex centers in the later images. This is typical of Lagrangian chaos (and chaotic systems in general): the phase space – real space in this case – is divided into ordered and chaotic regions, and any tracers initially in one of these regions will not cross into the other. The boundaries between the ordered and chaotic regions are therefore transport barriers.[2]

[2] A hole develops in the center vortex as well, even though dye that is initially within an ordered region should never leave. The cause of this hole is a weak, three-dimensional secondary flow that carries fluid up through the vortex centers. In this experiment, the dye that was injected into the center vortex was initially primarily near the top of the fluid layer, so the secondary flow circulated clear fluid up from below.

Quantitatively, a complete description of this process requires solution to the advection-diffusion equation:

$$\partial c / \partial t = D\nabla^2 c - \vec{u} \cdot \vec{\nabla} c \,, \tag{5}$$

where *c(x,y,t)* is the concentration field, $\vec{u}$ is the velocity field describing the oscillating vortex chain, and *D* is the molecular diffusion coefficient. Equation (5) cannot be solved in general, so other techniques must be used to analyze transport in the presence of fluid flows in general, and in situations with Lagrangian chaos in particular.

In advection-diffusion processes, it is common to consider the long-time growth of the variance of the concentration field and compare this growth to a power law of the form:

$$< r^2 > \sim t^{\gamma} . \tag{6}$$

If $\gamma = 1$, then the process is termed "normal" (although enhanced) diffusion, in which case Equation (5) is approximated by the effective diffusion equation:

$$\partial c / \partial t = D^* \nabla^2 c \,, \tag{7}$$

where D^* is the effective diffusion coefficient. Previous experiments [9,11] have shown that at many typical frequencies in this system, the transport can be approximated quite well by normal diffusion with an effective diffusion coefficient that grows linearly with the oscillation amplitude *B* for small *B*.

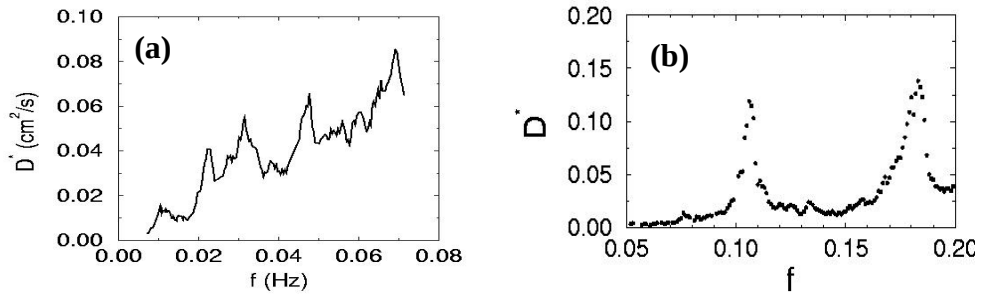

FIGURE 4. Simulations of the frequency dependence of the long-time limit of the enhanced diffusion coefficient D^*. (a) No-slip boundary conditions; (b) free-slip boundary conditions.

The dependence of D^* on the oscillation frequency $f = \omega/2\pi$ is significantly more complicated. Numerically [12], the dependence is dominated by well-defined resonance peaks, as seen in Fig. 4. (Experimentally, it is very difficult to map out the frequency dependence because of the extreme sensitivity to small changes in *f*.) Furthermore, for the frequencies near the resonance peaks, there is a transient period of superdiffusion where the variance grows faster than linearly – $\gamma > 1$ – although the long-time behavior is still diffusive ($\gamma = 1$). The duration of the transient gets longer

and longer the closer the frequency is to one of the resonant frequencies; in fact, it has been shown theoretically [13] that the *long-time* behavior is superdiffusive precisely at these resonant frequencies.

The explanation for these resonance peaks is found by considering the motion of individual tracers in the flow. For most frequencies, Lagrangian chaos results in particle trajectories that have the appearance of random, Brownian-like (diffusive) motion, as seen in Fig. 5(a) for the case with $f = 0.095$. For frequencies near the resonance peaks, however, the trajectories include long "flights" (jumps), some as long as tens or even hundreds of vortex widths, as seen in the $f = 0.106$ case in Fig. 5(a). Quantitatively, these jumps can be described by a Lévy distribution [14,15]

$$p(L) \sim L^{-\mu}, \tag{8}$$

with $2 < \mu < 3$, as seen in Fig. 5(b). This power law behavior is valid up to a cut-off length that grows (and presumably diverges) as the frequency nears the resonant value.

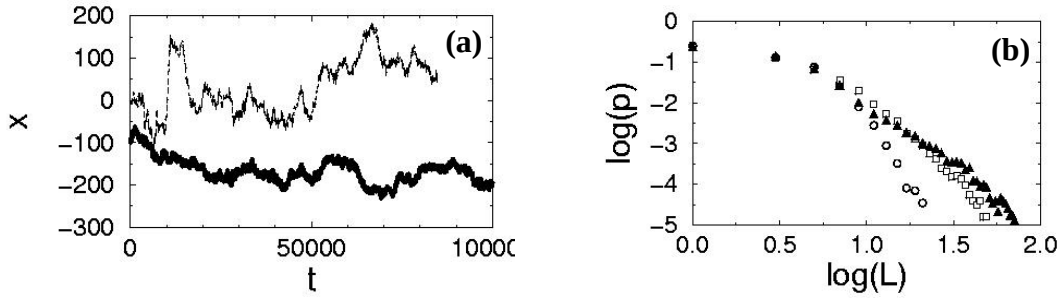

FIGURE 5. Evidence of Lévy flights in the free-slip simulations. (a) Sample trajecotories. The lower curve corresponds to a frequency $f = 0.095$, away from the resonance peaks. The upper curve corresponds to $f = 0.106$, near one of the resonance peaks. (b) Probability distribution functions for the flight lengths L. The frequencies are $f = 0.106$ (filled triangles), 0.103 (open squares), and 0.095 (open circles).

It has been well-established [16-20] that if tracers follow trajectories with flights that scale as in Equation (8) that the transport will be superdiffusive. In this situation, the transport is superdiffusive only for a transient period, consistent with the fact that the flights follow a Lévy distribution only up to a maximum length. The cause of the (truncated) Lévy flights is a resonance between the period of oscillation and typical times for fluid elements to circulate within a vortex, as shown in the cartoon in Fig. 6. At these resonant frequencies, a tracer that has crossed from one vortex to another loops around and finds itself at the opposite corner just at the right time to cross over again. The result is a snake-like trajectory which crosses several vortices in a short period of time. Another way of explaining these flights is with the use of "tangle islands" [21] that appear within the chaotic regions (inside the lobes) for frequencies near the resonant ones [12].

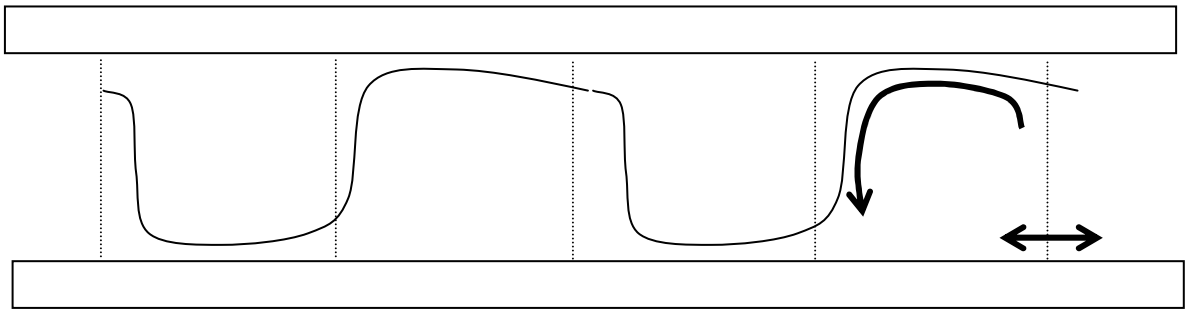

FIGURE 6. Cartoon showing resonance between circulation times and oscillation periods, responsible for the flights.

We have, then, a system where the transport can be either diffusive or (transiently) superdiffusive, depending on the frequency of oscillation.

LAGRANGIAN CHAOS AND COUPLED CHEMICAL OSCILLATORS

Up to this point, we have been discussing kinematical issues; namely, given a flow and some impurities, we have discussed how the impurities move in the flow. But Lagrangian chaos can have a significant effect on *dynamical* processes as well. Different scenarios are possible: (a) The velocity field itself can be partially advected with the flow (although it is more common to discuss advection of vorticity, which is derived from the velocity field), in which case the transport can feed back onto the flow itself. (b) There could be interactions between the various impurity molecules causing deviations from the advection-diffusion equation (Eq. 5). For instance, if the impurity and the surrounding fluid are immiscible, surface tension can inhibit the amount by which the impurity can be stretched by the flow. (c) The "concentration" field might be an active, reacting field, rather than a passive field that is merely advected. This last situation classifies as an advection-diffusion-reaction problem, which can be described by the equation

$$\partial c / \partial t = D\nabla^2 c - \vec{u} \cdot \vec{\nabla} c + f(c), \qquad (9)$$

where *f(c)* is some function denoting reaction of the impurity either with itself of with some additional chemicals in the system.

We have initiated experimental studies of advection-diffusion-reaction processes in the oscillating vortex flow. Specifically, we are looking at dynamics of the Belousov-Zhabotinsky (BZ) chemical reaction [22-25] in the flow and how the global behavior of the system is affected by Lagrangian chaos.

The procedure is quite straightforward: the apparatus is filled initially with chemicals typically used to demonstrate the BZ reaction in its oscillatory state[3]. Using ferroin as an indicator, the reaction oscillates between a red and blue color. The typical oscillation period for this mixture in a well-stirred batch reactor is about 40-50 seconds. The CCD video camera used for the imaging is fitted with a blue filter; consequently, in all the images, the blue phase appears white while the red phases appear black.

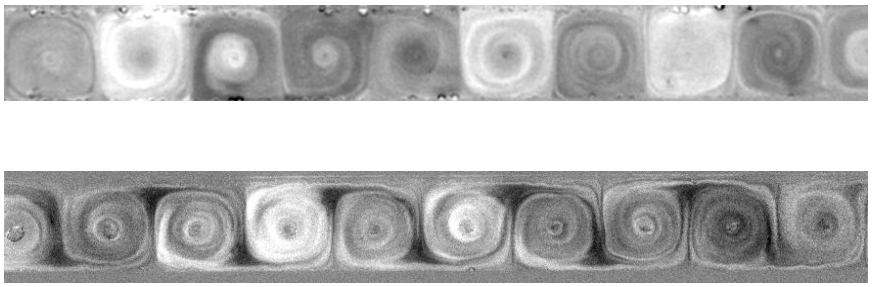

FIGURE 7. Snapshots of network behavior. In all cases, white (dark) regions correspond to the blue (red) phase of the BZ reaction. (a) Time-independent flow; no Lagrangian chaos. The chemical reactions in the vortices oscillate independently of each other. (b) Time-periodic forcing, small amplitude (b = 0.1), resonant frequency for lateral oscillations (f = 0.050 Hz). Lobe structures are clearly seen marked by the red (dark) phase of the BZ reaction.

The behavior of the network in the absence of any time dependence is shown in Figs. 7a and 8a. Since there is no Lagrangian chaos for the time-independent flow, the only communication between vortices is via molecular diffusion, a very weak mixing mechanism. Initially (before the starting time in Fig. 8a), the chemical oscillations in the different vortices are in phase since the system is initially well mixed (from pouring the fluid into the system). But after a moderate amount of time, the oscillations drift with respect to each other, as seen both in snapshots (Fig. 7a) and in a space-time plot (Fig. 8a). This drifting can be used to determine a characteristic "coherence time" τ_c, which is on the order of 400 s.

[3] The solution used in the experiments is composed of 400 ml of 1M sulfuric acid, 11.44 g of malonic acid, 4.18 g of potassium bromate, 0.44 g of cerium ammonium nitrate and 4 ml of 0.025 M ferroin.

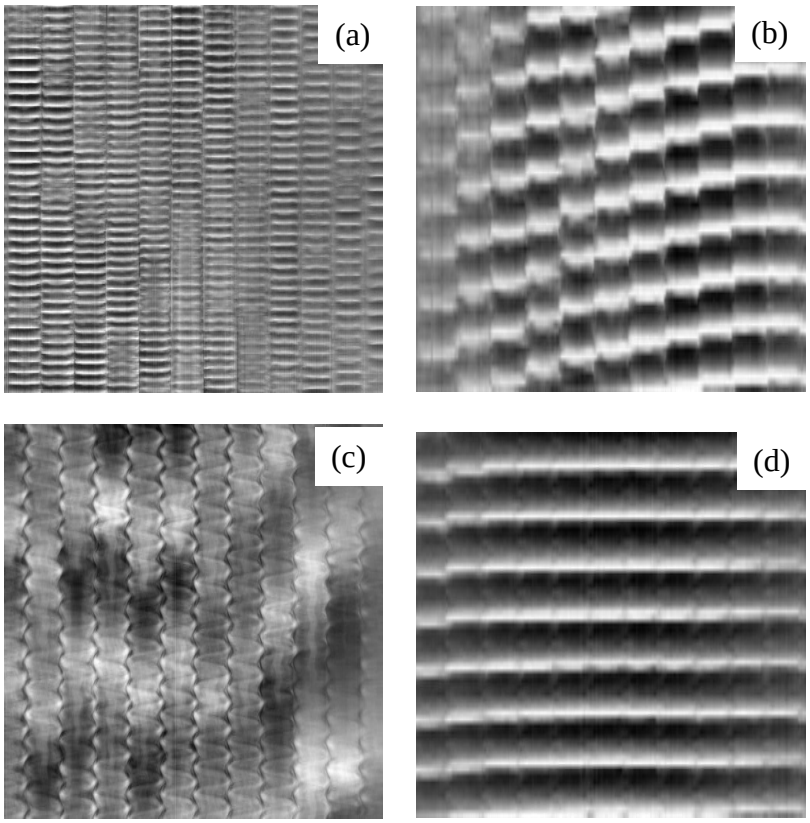

FIGURE 8. Space-time plots showing the dynamics of the networks; the horizontal direction is the distance across the vortex chain, and the vertical direction is time. (a) Time-independent flow (same conditions as Fig. 2a). (b) Time-periodic flow; small amplitude (b = 0.1), f = 0.037 Hz. (c) Time-periodic flow; small amplitude (b = 0.1), f = 0.050 Hz. (d) Time-periodic flow; larger amplitude (b = 0.2), f = 0.050 Hz. Total time spanned is 2500 s for (a) and 300 s for the other three.

For studies of the dynamics with time-periodic (lateral) oscillations, two different initial conditions are used: (1) Initially-synchronized: the entire apparatus is swept, mixing the contents of the entire vortex chain and starting off all the vortices with the same phase. (2) Initially unsynchronized: the oscillations are allowed to proceed for the time-independent flow until the oscillations are out of phase, after which the time-dependent forcing is turned on. The results presented here are preliminary.

At most frequencies studied, if the oscillations start out synchronized, they drift in phase and become unsynchronized within 20 periods of oscillation. If the pattern starts out unsynchronized, it tends to remain that way at these frequencies. In many cases, patterns will appear within vortices that are clear ghosts of the lobe structure seen in the passive transport. (Compare Figure 7b with Figure 3.) In studies of transport of dye in this flow, the lobes are only visible for a short period of time; basically, as long as there are strong concentration gradients. For the network of coupled chemical oscillations presented here, though, it is quite remarkable that the lobes remain visible indefinitely as *all* the lobes are tagged (and remain tagged) with the same chemical phase. Figure 8c shows a space-time plot for the same conditions

as Fig. 7b; the lobes can be seen in this plot as dark oscillatory structures within the vortices but synchronized throughout the chain.

At a couple of well-defined frequencies, the system synchronizes forming global traveling waves, as seen in Figure 8(b). These traveling waves appear regardless of whether the system starts as initially synchronized or unsynchronized. At these frequencies, traveling waves are observed propagating left-to-right, right-to-left, outward from a source in the middle of the vortex chain and inward toward the middle. And in a couple of the experimental runs, the system remained globally-synchronized (each vortex oscillating almost perfectly in phase) for 60 oscillation periods.

DISCUSSION

In analyzing the results of the advection-reaction-diffusion experiments described in the previous section, it is necessary to consider transport effects, since coupling between the vortices is determined by transport of the contents between vortices. As discussed earlier in this article, at most frequencies transport in the vortex chain is diffusive (although enhanced). In the vicinity of certain well-defined frequencies, though, the transport is characterized by transient superdiffusion and flights. If we think of our system as a network, then comparisons can be made between regular and "small world" networks discussed in recent studies [26]. The main ideas are illustrated in Figure 9 below:

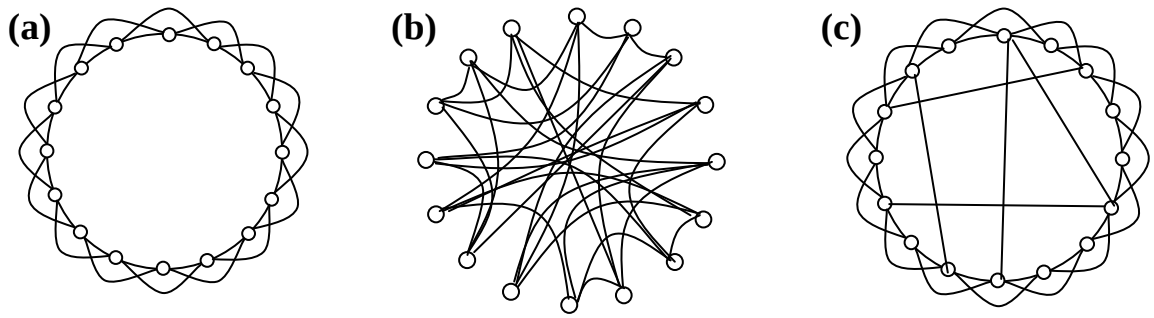

FIGURE 9. Coupling scenarios for networks. (a) Regular, nearest-neighbor coupling. (b) Random coupling. (c) "Small-world" coupling of Watts and Strogatz.

Figure 9(a) shows regular, nearest-neighbor coupling where each node is connected to one or two of its nearest neighbors but does not communicate with any other node directly. This type of coupling leads to "clustering" where local groups of nodes tend to have similar behavior. By contrast, in a randomly-coupled network (Fig. 9b), clustering is not observed; however, this type of network has a property referred to as the "Small World Effect" whereby the number of jumps needed – on the average – to connect any two arbitrary nodes grows logarithmically with the total number of nodes (rather than growing linearly). A third type of network was proposed recently by Watts and Strogatz [26] which captures both clustering and the small-world effect with a mostly-regular network with a few random "short-cut" connections.

Much has been said about these types of network connections, and these classifications have been applied to a wide variety of network systems. But little is known about the effects of these different coupling schemes on the *dynamics* of processes occurring on these networks. The experiments presented here on coupled chemical oscillations in an oscillating vortex chain might provide an experimental system whereby the effects of coupling schemes on the dynamics can be investigated. The coupling here is via transport, which at most frequencies is diffusive, which is inherently a nearest-neighbor coupling mechanism (mixing occurs primarily between adjacent vortices). On the other hand, at or near the resonant frequencies for transient superdiffusion, the flights that appear allow mixing between distant vortices in a short period of time. These flights are, in some sense, analogous to the short-cuts in the Watts/Strogatz small-world model

As to whether the difference in the observed dynamics from the previous section can be explained from this framework, the results are still inconclusive, and more data is needed. In particular, the frequencies for the traveling waves and globally-synchronized states need to be compared carefully with the frequencies for the peaks in the long-term effective diffusion coefficient. These experiments are currently in progress.

In modeling the behavior, the time scales for mixing in this experiment need to be considered. Specifically, how fast must mixing occur to enable synchronization? The longest flight time (from one end of the network to the other) is approximately 100 seconds, whereas typical circulation times are approximately 20 s. The period of the chemical oscillation is around 40 s, which is shorter than the longest flight times. However, our conjecture is that the relevant time scale is the coherence time 400 s, discussed earlier, which is significantly longer than all of the mixing timescales. Furthermore, the model of Ref. 1 needs to be modified, since Lévy flights can connect every vortex with every other vortex, but with a probability distribution that depends both on the separation between the vortices and also on the size of the portion of the chaotic region that gives rise to flights.

ACKNOWLEDGMENTS

This work was supported by the US National Science Foundation (grants DMR-0071771 and REU-0097424).

REFERENCES

1. Aref, H., *J. Fluid Mech.* **143**, 1 (1984).
2. Ottino, J.M., Leong, C. W., Rising, H. , and Swanson, P. D. , *Nature* **333**, 419 (1988).
3. Bolton, E. W., Busse, F. H., and Clever, R. M., *J. Fluid Mech.* **164**, 469 (1986).
4. Solomon, T. H. , and Gollub, J. P., *Phys. Rev. A* **38**, 6280 (1988).
5. Gollub, J. P., and Solomon, T. H., *Phys. Scripta* **40**, 430 (1989).
6. Solomon, T.H., *Transport and Boundary Layers in Rayleigh-Bénard Convection*, PhD thesis, 1990.
7. Chandrasekhar, S., *Hydrodynamic and Hydromagnetic Stability*, Dover (New York), 1961.
8. Willaime, H., Cardoso, O., and Tabeling, P., *Phys. Rev. E* **48**, 288 (1993).

9. Solomon, T.H., Tomas, S., and Warner, J. L., *Phys. Rev. Lett.* **77**, 2682 (1996).
10. Rom-Kedar, V., Wiggins, S., *Physica D* **51**, 248 (1991).
11. Solomon, T.H., Tomas, S., and Warner, J.L., *Phys. Fluids* **10**, 342 (1998).
12. Solomon, T.H., Lee, A.T., and Fogleman, M.A., *Physica D* **157**, 40 (2001).
13. Castiglione, P., Crisanti, A., Mazzino, A., Vergassola, M., and Vulpiani, A., *J. Phys. A* **31**, 7197 (1998).
14. B. D. Hughes, M. F. Shlesinger, E. W. Montroll, *Proc. Natl. Acad. Sci. USA* **78**, 3287 (1981).
15. M. F. Shlesinger, G. M. Zaslavsky, J. Klafter, *Nature* **363**, 31 (1993).
16. Shlesinger, M.F., *J. Stat. Phys.* **10,** 421 (1974).
17. Wang, W.-J., *Phys. Rev. A* **45**, 8407 (1992).
18. Klafter, J., and Zumofen, G., *Phys. Rev. E* **49**, 4873 (1994).
19. Solomon, T.H., Weeks, E.R., and Swinney, H.L., *Phys. Rev. Lett.* **71**, 3975 (1993).
20. Weeks, E.R., and Swinney, H.L., *Phys. Rev. E* **57**, 4915 (1998).
21. Rom-Kedar, V., and Zaslavsky, G., *Chaos* **9**, 697 (1999).
22. I. R. Epstein, *Physica D* **7**, 47 (1983).
23. R. A. Schmitz, K. R. Graziani, J. L. Hudson, *J. Chem. Phys.* **67**, 3040 (1977).
24. A. T. Winfree, *Science* **175**, 634 (1972).
25. K. Showalter, *J. Chem. Phys.* **73**, 3735 (1980).
26. D. J Watts, S. H. Strogatz, *Nature.* **393**, 440 (1998).